THE ASTROPHYSICAL JOURNAL, 302:421–431, 1986 March 1

COLORS OF REFLECTION NEBULAE. III. ULTRAVIOLET SCATTERING BY SMALL PARTICLES IN REFLECTION NEBULAE ASSOCIATED WITH 17, 20, AND 23 TAURI

ADOLF N. WITT[1]
Ritter Astrophysical Research Center, University of Toledo
RALPH C. BOHLIN[1]
Space Telescope Science Institute
AND
THEODORE P. STECHER[1]
Goddard Space Flight Center
Received 1985 June 27; accepted 1985 August 26

ABSTRACT

New surface brightness measurements in the reflection nebulae associated with the Pleiades stars 17, 20, and 23 Tau have been carried out with the *IUE* satellite. Each nebula was observed at two angular offsets south of the respective illuminating star. At the larger offsets (40″, 40″, and 60″, respectively) each nebula exhibits a flux distribution which rises much more steeply with decreasing wavelengths than the corresponding stellar spectrum. At the smaller offsets (20″) the nebular spectra are more similar to those of the stars and fail to show the steep rise at $\lambda < 2200$ Å. Independent observations of interstellar absorption lines as well as theoretical arguments by several previous authors lead to a model wherein the reflection nebulosity near the Pleiades stars is caused by a thin sheet of interstellar matter in front of the stars, at an approximate distance of a few $\times 10^{-2}$ pc. In the context of such a model the nebular spectra obtained near 17, 20, and 23 Tau can be understood only if the phase-function asymmetry of scattering declines with decreasing wavelengths throughout the spectral range. This result indicates that the role of scattering in the UV by particles in the 10^{-6} cm size range appears more important than is generally recognized by current models.

Subject headings: nebulae: reflection — stars: individual — ultraviolet: spectra

I. INTRODUCTION

The color difference between reflection nebulae and their respective illuminating stars results from the difference between the transfer histories of the nebular radiation and of the directly observed stellar light. In the visible part of the spectrum, the well-studied λ^{-1} wavelength dependence of the optical depth coupled with an essentially constant dust albedo produces the familiar result of reflection nebulae appearing bluer than their illuminating stars, at least at small offsets. In this series of papers (Witt 1985, hereafter Paper I; Witt and Schild 1985, hereafter Paper II) we are investigating conditions and individual cases, where the color difference between nebulae and stars deviates significantly from the values expected on the basis of the wavelength dependence of the optical depth alone. Such deviations can be caused by other wavelength-dependent dust properties, e.g., variations of the albedo or the phase-function asymmetry with wavelength, or even by intrinsic particle luminescence as observed at wavelengths $\lambda \geq 6000$ Å (Witt, Schild, and Kraiman 1984; Witt and Schild 1985).

For this study we have taken advantage of the ability of the *International Ultraviolet Explorer* (*IUE*) satellite to conduct spectrophotometric observations in the UV at very small offset angles adjacent to a bright stellar source. This is of particular importance in the case of the Pleiades reflection nebulae, because the analysis of observations of interstellar absorption lines seen toward the Pleiades stars by Jura (1977, 1979), Federman (1982), and Freeman and Williams (1982) has provided convincing arguments suggesting that the interstellar gas seen in the line of sight to the Pleiades is located in a thin sheet within a small fraction of a parsec *in front* of the stars. Most recently, a comprehensive study by White (1984*a*, *b*) has confirmed and further elaborated the basic model suggested by the earlier authors. In particular, White has shown that the interstellar matter seen toward the Pleiades is concentrated in two sheets, one with atomic gas located more than 1 pc in front of the major cluster stars and one with molecular gas and most of the line-of-sight dust located 10^{-1}–10^{-2} pc in front of the stars. For dust associated with the latter sheet, one can expect significant changes of scattering angle to occur for small angular offsets on the sky. Therefore, these *IUE* observations have the potential of uncovering a wavelength dependence of the scattering phase function, when nebular spectra from positions with different offsets are compared. The presence of phase-function effects observable at small offsets would provide an independent confirmation of the existence of dust within a small fraction of a parsec of the stars, and thus of the coexistence of dust with the gas responsible for the absorption lines. Jura (1977) has shown that an optically thin layer [$E(B-V) = 0.08$, 0.05, 0.03 for 23, 20, and 17 Tau, respectively) of dust can explain the nebular surface brightness observed near these stars.

In § II of this paper we give a detailed account of the observation and reduction procedure, followed by an analysis in

[1] Guest Observer with the *International Ultraviolet Explorer* (*IUE*) satellite, which is sponsored and operated by the National Aeronautics and Space Administration, the European Space Agency, and the Science Research Council of the United Kingdom.

TABLE 1

SUMMARY OF THE *IUE* DATA USED IN THIS STUDY

	IUE IMAGE NUMBERS			
OBJECT	SWP	LWR	POSITION	DATE
17 Tau (HD 23302)	7570	6549	...	1980 Jan 5
	7572	6550	...	1980 Jan 5
17 Tau nebula	7571 (40^m)	6548 (30^m)	7".6E, 18".5 S	1980 Jan 5
	7569 (240^m)	6571 (240^m)	15".2 E, 37" S	1980 Jan 5
20 Tau (HD 23408)	5982	5199	...	1979 Aug 21
	7574	6552	...	1980 Jan 6
20 Tau nebula	5983 (60^m)	5200 (38^m)	21" S	1979 Aug 21
	6023 (195^m)	5222 (180^m)	40" S	1979 Aug 21
23 Tau (HD 23480)	5969	5180	...	1979 Aug 21
	7577	6553	...	1980 Jan 6
23 Tau nebula	5968 (60^m)	5179 (60^m)	20" S	1979 Aug 21
	5980 (240^m)	5197 (240^m)	60" S	1979 Aug 21

NOTE.—Numbers in parentheses are exposure times.

terms of a first-order color-difference method in § III. The implications of the results will be discussed in § IV, and a summary is provided in § V.

II. OBSERVATIONS

In Table 1 the details of the *IUE* observations are given. All spectra were obtained in the low-resolution mode of the *IUE* spectrograph, and the SWP and LWR cameras were used to cover the spectral range $1250 \leq \lambda \leq 3150$ Å. The large oval apertures were used for all nebular exposures, with exposure times listed in parentheses following the corresponding image number in Table 1. The positioning of the three stars 17, 20, and 23 Tau *in the reference frame of the aperture plate* of the long-wavelength (LW) spectrograph is shown in Figure 1. After selecting the point of observation in the nebula, the orientation of the long axis of the long-wavelength large aperture (LWLA) with respect to the direction to the respective star is fixed by the roll angle of the spacecraft, which in turn is determined by the date of observation. Also shown as crossing the LWLA are the five central image scan lines of the spatially resolved extracted spectrum, which were used exclusively for the derivation of nebular intensities. The *IUE* large apertures are not exactly perpendicular to the dispersion direction. The tilt of the slit with respect to the dispersion is 81° for the SWP and 97° for the LWR. (Bohlin, Lindler, and Turnrose 1981). This approach was mandated mainly for two reasons: (1) some of the spectra taken at the smallest offsets had overexposed sections at the edge of the aperture facing the star, leaving only the central and lower portion as usable data, and (2) the study of the anticipated variation of the spectral shape of the nebular spectra required precise spatial definition, which might have been lost by averaging over the entire aperture.

The reduction procedure was as follows: After processing, which incorporated corrections to the reseau positions based on the instrument temperatures recorded during the observations, the extracted line-by-line spatially resolved data were integrated over 100 Å wide bandpasses. The camera back-

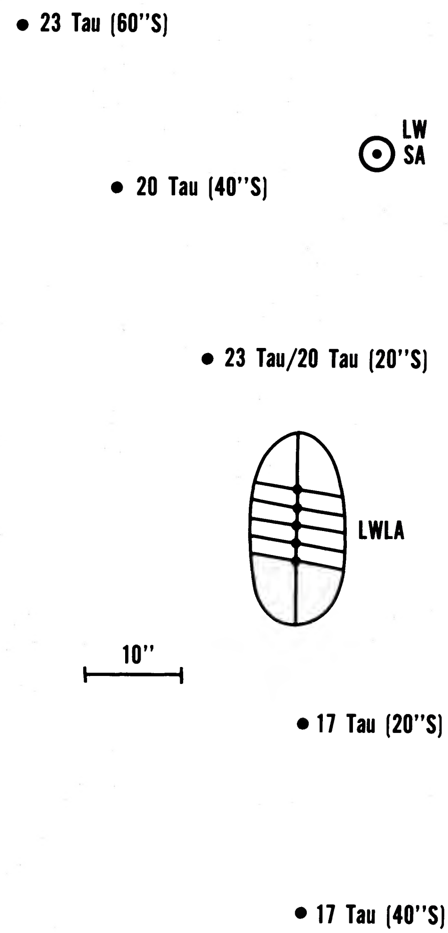

FIG. 1.—Positions of the three stars 17, 20, and 23 Tau in the fixed reference frame of the aperture plate of the long-wavelength (LW) *IUE* spectrograph during the nebular exposures listed in Table 1. Crossing the LW large aperture at the angle of 97° are the five central image scan lines of the spatially resolved extracted spectrum used for the derivation of the nebular spectrum.

TABLE 2

IUE RESULTS FOR THE 23 TAURI (Merope) NEBULA

		20″ SOUTH		60″ SOUTH	
λ (Å)	log F_*[a]	log S[b]	log (S/F_*)[c]	log S[b]	log (S/F_*)[c]
1300......	−9.47	-4.18 ± 0.05	5.29	-4.70 ± 0.02	4.77
1400......	−9.40	-4.21 ± 0.03	5.19	-4.70 ± 0.02	4.70
1500......	−9.39	-4.22 ± 0.01	5.17	-4.72 ± 0.02	4.67
1600......	−9.46	-4.31 ± 0.02	5.15	-4.79 ± 0.03	4.67
1700......	−9.51	-4.38 ± 0.03	5.13	-4.88 ± 0.02	4.63
1800......	−9.52	-4.40 ± 0.02	5.12	-4.93 ± 0.02	4.59
1900......	−9.60	-4.43 ± 0.03	5.17	-5.01 ± 0.02	4.59
2000......	−9.63	-4.46 ± 0.03	5.17	-5.14 ± 0.03	4.49
2100......	−9.69	-4.48 ± 0.05	5.21	-5.20 ± 0.03	4.49
2200......	−9.75	-4.60 ± 0.05	5.15	-5.29 ± 0.02	4.46
2300......	−9.77	-4.68 ± 0.03	5.09	-5.31 ± 0.03	4.46
2400......	−9.78	-4.75 ± 0.03	5.03	-5.39 ± 0.02	4.39
2500......	−9.76	-4.80 ± 0.04	4.96	-5.40 ± 0.02	4.36
2600......	−9.77	-4.79 ± 0.04	4.98	-5.39 ± 0.02	4.38
2700......	−9.79	-4.84 ± 0.03	4.95	-5.45 ± 0.02	4.34
2800......	−9.81	-4.83 ± 0.05	4.98	-5.47 ± 0.03	4.34
2900......	−9.81	-4.83 ± 0.04	4.98	-5.51 ± 0.03	4.30
3000......	−9.81	-4.88 ± 0.05	4.93	-5.55 ± 0.04	4.26
3100......	−9.85	-4.87 ± 0.05	4.98	-5.55 ± 0.04	4.30

[a] Units: ergs cm^{-2} s^{-1} Å^{-1}.
[b] Units: ergs cm^{-2} s^{-1} Å^{-1} sr^{-1}.
[c] Units: sr^{-1}; standard deviations are same as for corresponding log S.

ground was defined by lines 11–20 and 37–46, with the spectrum contained within lines 24–32. As indicated above, only lines 26–30 were used for the derivation of observed intensities, and their net signal was found by subtracting the linearly interpolated background from the gross signal.

A major correction was applied for instrumental scattering resulting from the presence of the illuminating star image near the spectrograph aperture. The correction procedure described by Witt *et al.* (1982) was used here. The steep radial gradient of the instrumentally scattered light implies that the corrections at the smallest offsets (20″) were most severe and are therefore a major source of uncertainty for the final nebular intensities. For example, at 20″ offset from Merope, only about 50% of the signal recorded with the SWP camera and between 47% and 33% of that recorded with the LWR camera is due to nebular light, while at 60″ offset, between 85% and 75% of the total is nebular signal. At the intermediate offset of 40″ in the case of 20 Tau, between 75% and 45% of the total signal is due to the nebula. The worst case is that of 17 Tau, where at 20″ offset only 22%–26% of the signal is of nebular origin. We have applied our scattered-light corrections with confidence, however, because the observations upon which these corrections are based were taken with the bright star η UMa in the same relative positions with respect to the large aperture as those of the illuminating stars 17, 20, and 23 Tau.

In Tables 2, 3, and 4 we summarize the results for the nebular intensity S and the relative surface brightness S/F_*, where F_* is the flux of the respective illuminating stars, averaged over the same 100 Å wide bandpasses. Values of F_* were obtained from the stellar exposures with the *IUE* listed in Table 1.

III. ANALYSIS

a) Comparison with Existing Observations

We can compare the consistency of our results both internally and in comparison with other published observations. The 23 Tau (Merope) nebula has not previously been observed at offsets as small as reported here, but UV surface brightness data at 1550, 1800, 2200, 2500, and 3300 Å exist for a large range of greater offsets from the measurements by Andriesse, Piersma, and Witt (1977) with the *Astronomical Netherlands Satellite* (*ANS*). In Figure 2 we show these data for 1550 and 2500 Å, together with our *IUE* results for the Merope nebula at 60″ and at 20″ offset. Our new data appear to extend the well-defined surface brightness distributions delineated by the *ANS* results into the immediate vicinity of 23 Tau. At 1550 Å the surface brightness of this nebula has now been measured over more than 2 orders of magnitude in intensity, and the uniformity of the surface brightness distribution speaks to the essential simplicity of the structure of this nebula.

For the 20 Tau (Maia) and the 17 Tau (Electra) nebulae there exist *uvby* surface brightness measurements at 50″ offset south of the respective stars from the work of Cottrell and Witt (1983), albeit with a much larger aperture. The *u* filter with an effective wavelength near 3470 Å is close enough in wavelength to be compared with the long-wavelength end of the *IUE* spectral range. A 63″ circular aperture centered 50″ south of 20 Tau, but averaging the nebular intensity over an offset range 18″.5 ≤ 81″.5, yielded log $(S/F_*)_u = 4.26$, while a similar average over the offset range $25 \leq r \leq 75''$ produced log $(S/F_*)_u = 4.22$. Our values of 4.2–4.3 at 40″ and 4.6–4.7 at 20″ for the 2700 Å $\leq \lambda \leq$ 3100 Å range with a much smaller aperture are consistent with these results. A similar comparison for the data on the 17 Tau (Electra) nebula is equally satisfactory.

Finally, we find that the ratios of the relative surface brightness at 20″ among the three nebulae studied equal the ratios of the optical depths implied by the observed color excesses $E(B - V) = 0.08$, 0.05, and 0.03 for the respective stars. The nebulosity near the stars is consistent with scattering in an optically thin layer located *in front of* the stars, implying a similar structure at small offsets for all these nebulae. Addi-

TABLE 3

IUE RESULTS FOR THE 20 TAURI (Maia) NEBULA

		20″ SOUTH		40″ SOUTH	
λ (Å)	log F_*[a]	log S[b]	log (S/F_*)[c]	log S[b]	log (S/F_*)[c]
1300......	−9.32	-4.42 ± 0.05	4.90	-4.66 ± 0.03	4.66
1400......	−9.31	-4.36 ± 0.04	4.95	-4.64 ± 0.03	4.67
1500......	−9.28	-4.35 ± 0.04	4.93	-4.66 ± 0.03	4.62
1600......	−9.38	-4.42 ± 0.03	4.96	-4.72 ± 0.04	4.66
1700......	−9.42	-4.42 ± 0.04	5.00	-4.82 ± 0.03	4.60
1800......	−9.44	-4.46 ± 0.02	4.98	-4.87 ± 0.02	4.57
1900......	−9.52	-4.43 ± 0.05	5.09	-4.91 ± 0.02	4.61
2000......	−9.52	-4.59 ± 0.03	4.93	-5.02 ± 0.03	4.50
2100......	−9.59	-4.63 ± 0.05	4.94	-5.11 ± 0.02	4.46
2200......	−9.65	-4.72 ± 0.10	4.93	-5.22 ± 0.03	4.43
2300......	−9.67	-4.80 ± 0.12	4.87	-5.30 ± 0.03	4.37
2400......	−9.70	-4.87 ± 0.10	4.83	-5.36 ± 0.04	4.34
2500......	−9.67	-4.86 ± 0.08	4.81	-5.34 ± 0.03	4.33
2600......	−9.67	-4.89 ± 0.06	4.78	-5.34 ± 0.03	4.33
2700......	−9.69	-4.96 ± 0.10	4.73	-5.38 ± 0.03	4.31
2800......	−9.71	-5.00 ± 0.10	4.71	-5.41 ± 0.04	4.30
2900......	−9.69	-4.98 ± 0.10	4.71	-5.44 ± 0.03	4.25
3000......	−9.69	-5.09 ± 0.15	4.60	-5.47 ± 0.03	4.22
3100......	−9.71	-5.11 ± 0.15	4.60	-5.56 ± 0.08	4.15

[a] Units: ergs cm^{-2} s^{-1} Å^{-1}.
[b] Units: ergs cm^{-2} s^{-1} Å^{-1} sr^{-1}.
[c] Units: sr^{-1}; standard deviations are same as for corresponding log S.

tional support for this model comes from the fact that also at 40″ offset the 20 Tau and 17 Tau nebulae show a surface brightness ratio which is consistent with this model and which furthermore is in excellent agreement with the surface brightness ratios found at 50″ offset in *uvby* for these two nebulae by Cottrell and Witt (1983).

b) *Nebular Color Differences*

The relative surface brightness values listed in Tables 2, 3, and 4 in each case are a result of the line-of-sight distribution of the scattering dust and the wavelength dependences of the optical depth, the dust albedo, and the phase function. To model the surface brightness uniquely would require more information concerning the star-nebula geometry then is presently available. However, as demonstrated in Paper I, a discussion of color differences between nebula and star can reveal changes in the dust properties with wavelength without relying on information on the exact spatial geometry. The color difference was defined in Paper I as

$$\Delta C(\lambda_1, \lambda_2) = \log \frac{(S/F_*)_{\lambda_1}}{(S/F_*)_{\lambda_2}} . \qquad (1)$$

TABLE 4

IUE RESULTS FOR THE 17 TAURI (Electra) NEBULA

		20″ SOUTH		40″ SOUTH	
λ (Å)	log F_*[a]	log S[b]	log (S/F_*)[c]	log S[b]	log (S/F_*)[c]
1300......	−9.10	-4.46 ± 0.10	4.64	-4.66 ± 0.03	4.44
1400......	−9.11	-4.43 ± 0.10	4.68	-4.70 ± 0.03	4.41
1500......	−9.12	-4.40 ± 0.15	4.72	-4.74 ± 0.03	4.38
1600......	−9.20	-4.35 ± 0.15	4.85	-4.76 ± 0.03	4.44
1700......	−9.25	-4.46 ± 0.15	4.79	-4.92 ± 0.02	4.33
1800......	−9.25	-4.59 ± 0.15	4.66	-4.98 ± 0.03	4.27
1900......	−9.33	-4.79 ± 0.15	4.77	-5.05 ± 0.03	4.28
2000......	−9.35	-4.84 ± 0.15	4.56	-5.22 ± 0.05	4.13
2100......	−9.38	-4.84 ± 0.20	4.54	-5.26 ± 0.03	4.12
2200......	−9.44	-4.81 ± 0.10	4.63	-5.38 ± 0.06	4.06
2300......	−9.49	-4.76 ± 0.10	4.73	-5.38 ± 0.04	4.11
2400......	−9.53	-4.83 ± 0.10	4.70	-5.46 ± 0.03	4.07
2500......	−9.52	-4.80 ± 0.15	4.72	-5.54 ± 0.03	3.98
2600......	−9.53	-4.81 ± 0.15	4.72	-5.55 ± 0.04	3.98
2700......	−9.55	-4.84 ± 0.10	4.71	-5.57 ± 0.04	3.98
2800......	−9.58	-4.92 ± 0.15	4.66	-5.62 ± 0.10	3.96
2900......	−9.58	-4.95 ± 0.15	4.63	-5.75 ± 0.12	3.83
3000......	−9.59	-5.15 ± 0.20	4.44	-5.91 ± 0.15	3.68
3100......	−9.63	-5.17 ± 0.10	4.46	-5.95 ± 0.15	3.68

[a] Units: ergs cm^{-2} s^{-1} Å^{-1}.
[b] Units: ergs cm^{-2} s^{-1} Å^{-1} sr^{-1}.
[c] Units: sr^{-1}; standard deviations are same as for corresponding log S.

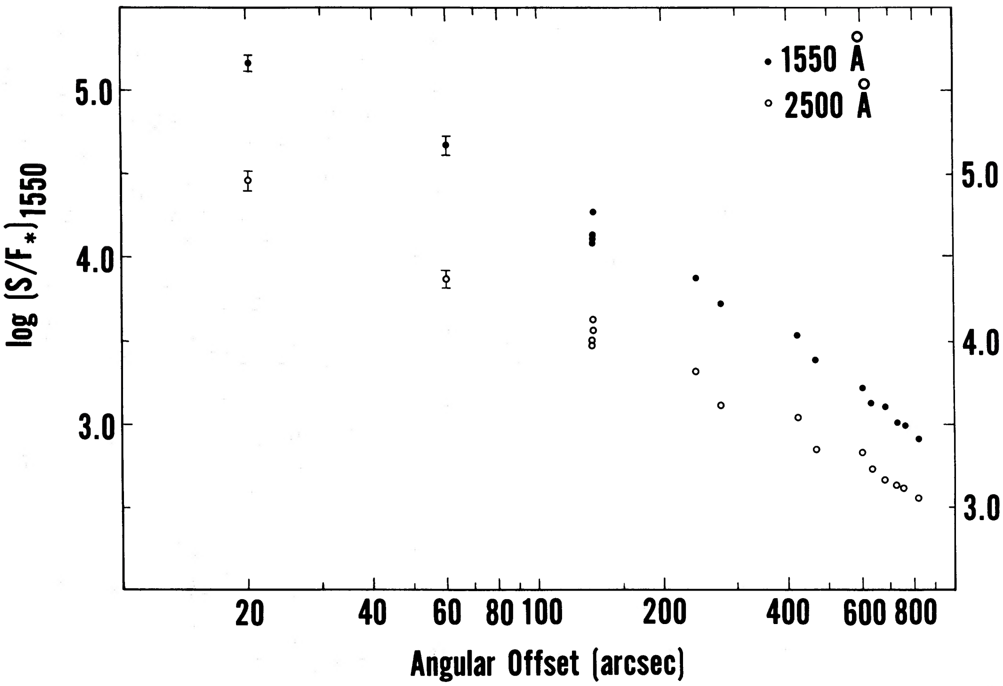

FIG. 2.—Surface brightness measurements as a function of offset angle for the Merope (23 Tau) nebula are shown for the effective wavelengths 1550 and 2500 Å. The new *IUE* results are shown as symbols with error bars. Note the displacement of the two vertical scales.

For an arbitrary geometry and to an approximation which included illuminating radiation from the star only,

$$\Delta C(\lambda_1, \lambda_2) \approx \log \frac{a(\lambda_1)[1 - e^{-\tau_0(\lambda_1)}]e^{\tau_*(\lambda_1) - \tau_1(\lambda_1)}}{a(\lambda_2)[1 - e^{-\tau_0(\lambda_2)}]e^{\tau_*(\lambda_2) - \tau_1(\lambda_2)}p(\lambda_1, \lambda_2)} . \quad (2)$$

The dust characteristics are represented by the albedo ratio $a(\lambda_1)/a(\lambda_2)$ and the phase contribution ratio p defined as

$$p(\lambda_1, \lambda_2) = \frac{\int_{\alpha_1}^{\alpha_2} \Phi[\alpha, g(\lambda_2)] \sin^2 \alpha d\alpha}{\int_{\alpha_1}^{\alpha_2} \Phi[\alpha, g(\lambda_1)] \sin^2 \alpha d\alpha} . \quad (3)$$

The latter quantity couples the nebular geometry with the scattering phase function Φ through the scattering angle $\alpha_1 < \alpha < \alpha_2$. We have $p \neq 1$, if Φ is wavelength dependent. The dust distribution in optical depth space is defined by the quantities $\tau_0(\lambda)$, the line-of-sight optical thickness of the nebula; $\tau_*(\lambda)$, the optical depth of nebular material in front of the star in the direction to the observer; and $\tau_1(\lambda)$, a suitably averaged optical depth between the illuminating star and the scattering volume observed.

In Figure 3 we are comparing the wavelength dependence of log (S/F_*) observed at 60″ south of 23 Tau (Merope) with predicted color differences derived from equation (2), normalized at $\lambda_2 = 2740$ Å. The solid curve is based on the wavelength dependence of extinction found by Witt, Bohlin, and Stecher (1981) for the Pleiades member HD 23512, while the dashed and dotted curves use the average interstellar extinction law of Savage and Mathis (1979) to yield the wavelength dependence of the optical depth. The dashed as well as the solid curve are based on the assumption that the star is situated behind a dust layer of $\tau_V = 0.24$, while the dotted curve assumes such a layer both in front of and in back of the illuminating star. For all calculations the ratio $Q = a(\lambda_1)/[a(2740 \text{ Å})p(\lambda_1, 2740 \text{ Å})]$ has been taken as unity, with the expectation that deviation of observations from the model computed with this simple assumption will reveal the actual wavelength dependence of Q. Figure 3 suggests that Q is greater than unity for $\lambda < 2200$ Å, if we base our comparison on the solid curve derived from the more appropriate Pleiades reddening law. In the 1900 Å $> \lambda >$ 1500 Å region we find $Q \approx 1.5$ at 60″ offset.

Figure 4 shows the same comparison for the data obtained 20″ south of 23 Tau (Merope). Immediately noticeable is the very different shape of the nebular spectrum when compared with that at 60″ offset: the far-UV portion has lost its steep blue characteristics. The dependence of the spectral shape on offset indicates that the wavelength variation of the ratio Q is mainly determined by $p(\lambda_1, 2740 \text{ Å})$, because a wavelength-dependent albedo ratio $a(\lambda)/a(2740 \text{ Å})$ would affect the nebular spectrum in an *offset-independent* manner, assuming uniform dust properties. The findings for the two offsets in the Merope nebula are qualitatively repeated in the comparison of the Maia data at 40″ and 20″ offset (Figs. 5 and 6) and in the Electra data at 40″ and 20″ offset (Figs. 7 and 8). In Table 5 we are summarizing the Q-values found for five of the six cases. The case of 20″ south of Electra is subject to large uncertainties, and meaningful Q-values cannot be found, except that $Q < 1$ is a fair estimate for most of the UV region. The basis for comparison in each case is the predicted color curve derived from the Pleiades extinction curve.

A feature common to all three nebular spectra obtained at the larger offsets is an apparent excess in the 1600 Å bandpass, where the corresponding Q-values in Table 5 achieve maximum values. It is possible that these peaks are caused by H_2 fluorescence, predicted to occur in reflection nebulae by Duley and Williams (1980). We want to emphasize, however, that possible H_2 emission would be limited to a relatively

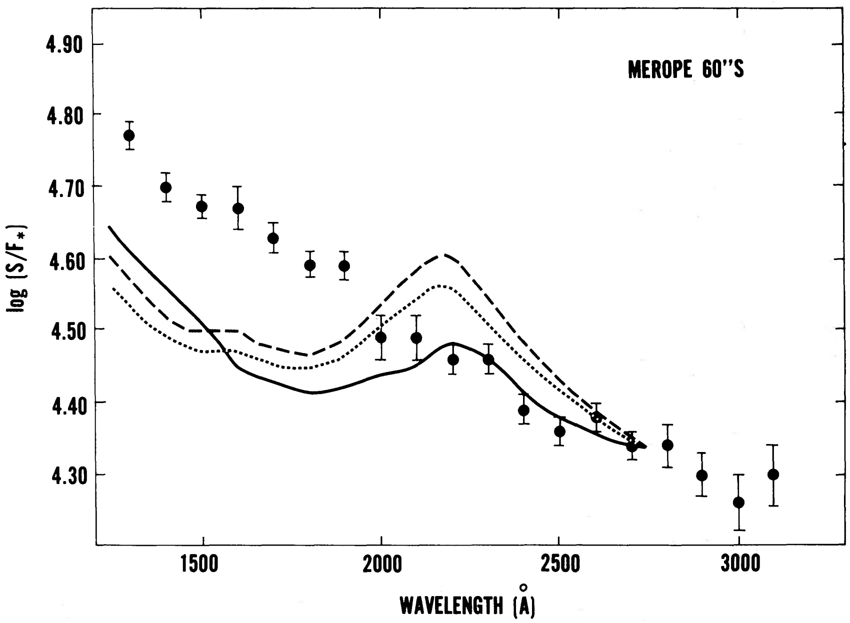

FIG. 3.—Comparison of the surface brightness of the Merope nebula observed 60″ south of 23 Tau with theoretically expected wavelength dependences of the color difference nebula minus star, normalized at 2740 Å. The theoretical curves are computed from eq. (2) with the assumptions $a(\lambda)/a(2740) = 1$ and $p(\lambda, 2740) = 1$. The solid curve is based on the UV reddening curve observed for the Pleiades, while the dashed curve is based on the average Galactic extinction law, with only dust *in front* of the stars taken into account. The dotted curve assumes the average Galactic extinction law with equal amounts of dust *in front* of and *behind* 23 Tau involved in the scattering.

narrow range of wavelengths around 1600 Å and cannot be invoked to explain the large Q-values found for the entire $\lambda <$ 2000 Å region.

c) *Where Is the Dust?*

If we are to understand the different nebular spectra at 20″ offset and at 40″ offset (60″ in case of Merope) in terms of phase-function effects, we must require that the effective scattering angles at the two offsets in question be markedly different. At the distance of the Pleiades (126 pc) the offset of 20″ corresponds to a linear offset in the Pleiades vicinity of 0.012 pc. Consequently, the distance d of the scattering dust from the illuminating stars must be of a similar order of magnitude.

Several independent arguments support this picture. The investigations of interstellar absorption lines seen toward the Pleiades stars, in particular the lines of H_2 and CH^+, which

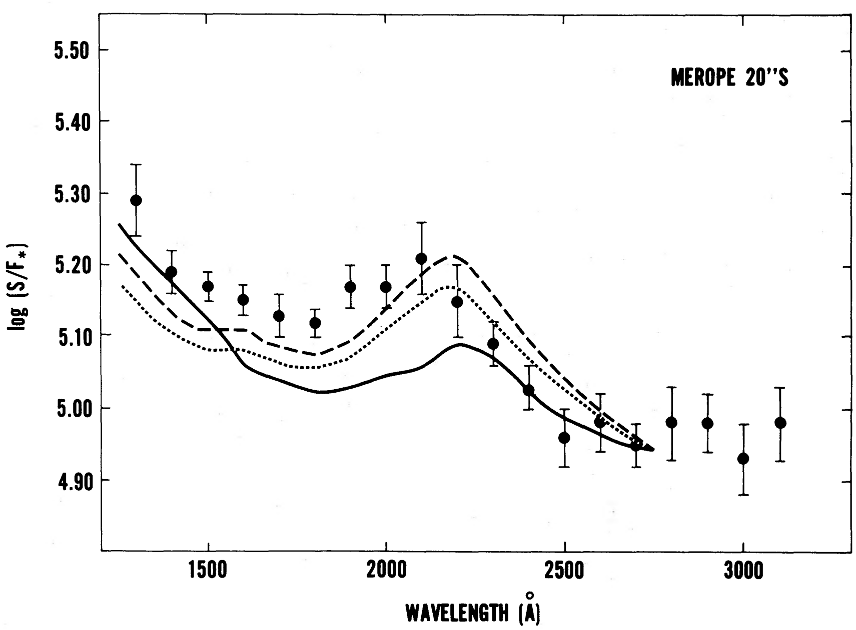

FIG. 4.—Same as Fig. 3, but for the location 20″ south of 23 Tau

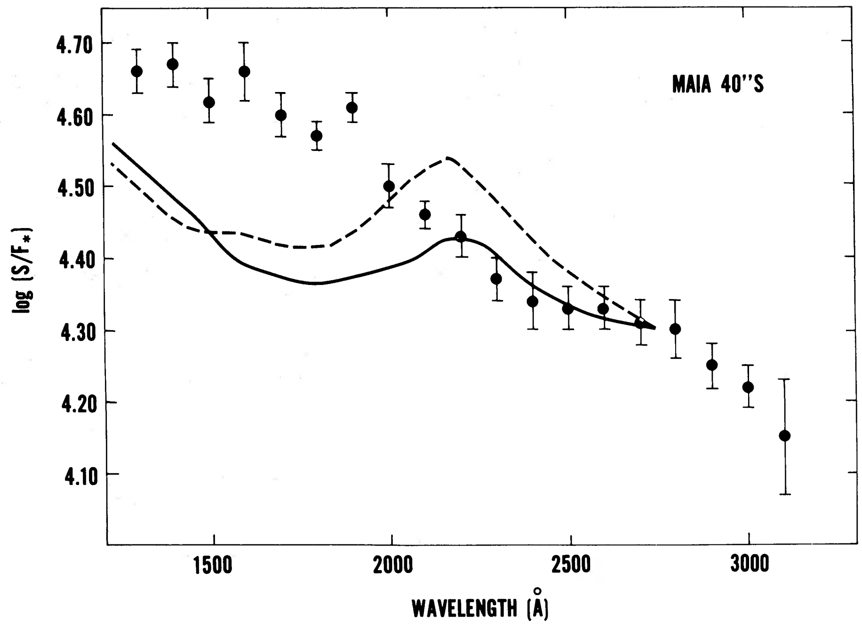

FIG. 5.—Same as Fig. 3, but for the location 40″ south of 20 Tau in the Maia nebula

were cited in § I, have resulted in a picture of a high-density, shocked gas sheet located at a distance anywhere from 0.3 pc (Federman) to 0.1 pc (Jura) to 0.05 pc (White) to 0.01 pc (Freeman and Williams) in front of the Pleiades stars. If we assume that the reflection nebulosity results from dust mixed with this gas sheet, we can obtain an estimate of its distance from the respective stars by using the formalism developed in Appendix A of Paper I. This yields

$$d = \left[\frac{F_*}{S}\, a(1 - e^{-\tau_0})e^{-\tau_1}e^{\tau_*}\,\frac{R^2}{4\pi}\right]^{1/2}, \tag{4}$$

and with the observed values at 20″ offset for $\lambda = 1500$ Å, we find $d \approx 7.25 \times 10^{-2}(a)^{1/2}$ pc, essentially unchanged for 17, 20, and 23 Tau. This is because $(1 - e^{-\tau_0})e^{-\tau_1}e^{\tau_*} \approx \tau_0$ for the assumed geometry and the small optical depths involved, and we have already found that $S/F_* \propto \tau_0$ for these nebulae. Consequently, for an albedo assumed as $a \approx 0.5$, we find $d \approx 0.05$ pc for all three cases.

The inferred presence of a shock front and the common dust distances suggest a common mechanism which has led to the formation of the dust sheets seen near these stars. One such mechanism would be the retarding effect of radiation pressure from the luminous Pleiades stars upon approaching dust (Arny

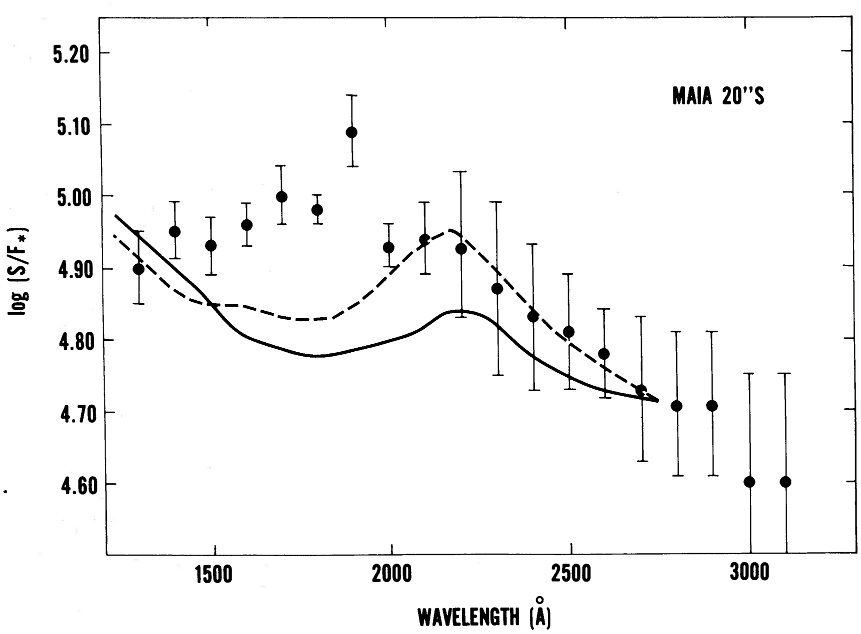

FIG. 6.—Same as Fig. 3, but for the location 20″ south of 20 Tau in the Maia nebula

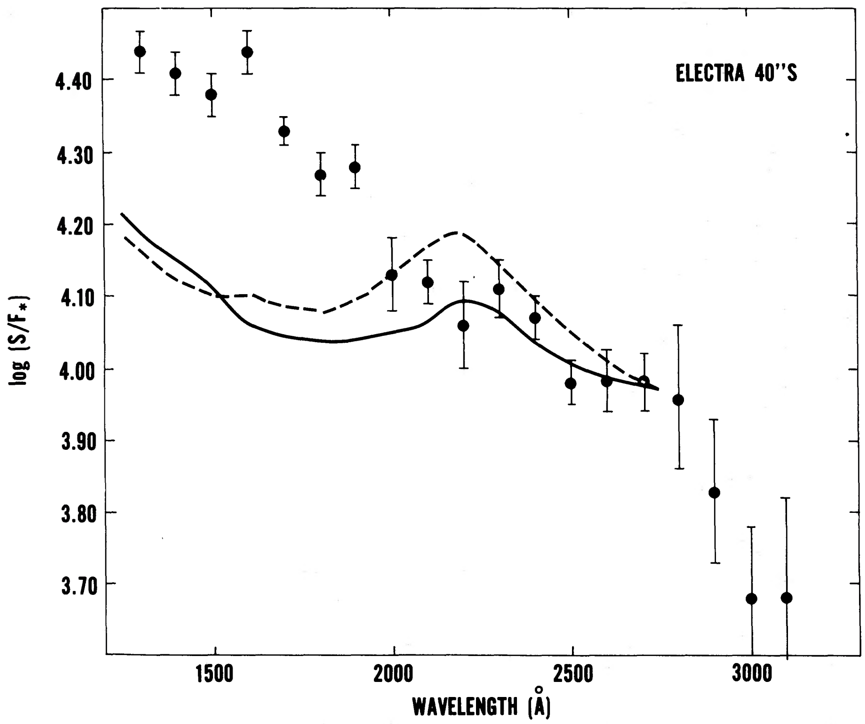

FIG. 7.—Same as Fig. 3, but for the location 40″ south of 17 Tau in the Electra nebula

1977; Bouvier 1982). Dust grains moving toward a star as part of an interstellar cloud would come to a standstill when a balance between radiation pressure and drag forces due to the supersonically streaming gas is achieved. From Martin (1978) we can estimate this distance as

$$d \approx \left(\frac{L_* \bar{Q}_r}{4\pi c n_g m_g u_{\mathrm{dr}}^2}\right)^{1/2}, \quad (5)$$

where $u_{\mathrm{dr}} \approx 10$ km s^{-1} is the drift velocity of the gas relative to the stationary grains. Gas parameters are given by the number density n_g and the average mass m_g of the gas particles. The average radiation pressure efficiency of the dust grains is given by $\bar{Q}_r$. With $L_* = 10^{36}$ ergs s^{-1}, $\bar{Q}_r \approx 0.5$, $n_g = 100$ cm^{-3}, $m_g = 3.34 \times 10^{-24}$ g, we find $d = 2 \times 10^{-2}$ pc.

Similarly, if we assume that a stellar wind from the Pleiades stars with a characteristic mass loss rate $\dot{m}_w = 10^{-8}\ M_\odot$ yr^{-1}

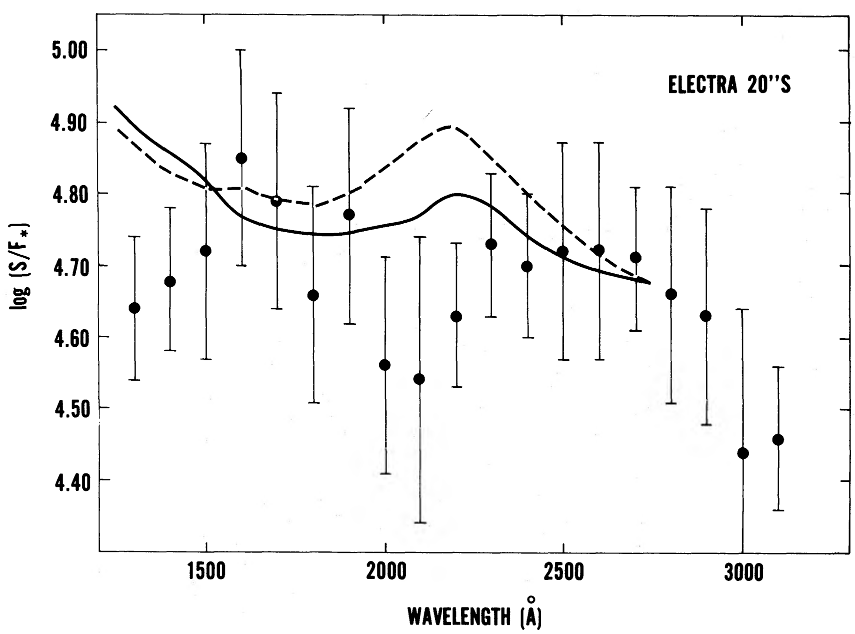

FIG. 8.—Same as Fig. 3, but for the location 20″ south of 17 Tau in the Electra nebula

TABLE 5

Q-VALUES FOR PLEIADES NEBULAE

	MEROPE		MAIA		ELECTRA
λ (Å)	60″ S	20″ S	40″ S	20″ S	40″ S
2500......	0.95 ± 0.05	0.91 ± 0.09	0.95 ± 0.05	1.12 ± 0.19	0.93 ± 0.07
2400......	0.95 ± 0.05	1.00 ± 0.07	0.91 ± 0.10	1.10 ± 0.25	1.10 ± 0.08
2300......	1.00 ± 0.03	1.02 ± 0.07	0.89 ± 0.08	1.10 ± 0.27	1.10 ± 0.10
2200......	0.95 ± 0.05	1.12 ± 0.03	0.98 ± 0.08	1.20 ± 0.25	0.93 ± 0.14
2100......	1.10 ± 0.08	1.38 ± 0.15	1.12 ± 0.04	1.32 ± 0.09	1.15 ± 0.08
2000......	1.12 ± 0.08	1.29 ± 0.09	1.27 ± 0.06	1.32 ± 0.09	1.20 ± 0.13
1900......	1.48 ± 0.07	1.38 ± 0.12	1.69 ± 0.08	2.00 ± 0.22	1.74 ± 0.12
1800......	1.51 ± 0.07	1.23 ± 0.06	1.69 ± 0.08	1.55 ± 0.07	1.70 ± 0.12
1700......	1.58 ± 0.07	1.20 ± 0.08	1.61 ± 0.08	1.58 ± 0.13	1.91 ± 0.09
1600......	1.66 ± 0.12	1.20 ± 0.05	1.79 ± 0.15	1.38 ± 0.09	2.40 ± 0.17
1500......	1.41 ± 0.07	1.07 ± 0.05	1.41 ± 0.09	1.12 ± 0.10	1.82 ± 0.12
1400......	1.35 ± 0.07	1.00 ± 0.07	1.47 ± 0.12	1.07 ± 0.09	1.78 ± 0.12
1300......	1.35 ± 0.07	1.07 ± 0.12	1.20 ± 0.06	0.81 ± 0.10	1.66 ± 0.12

and wind speed $v_w = 1000$ km s^{-1} interacts with incoming interstellar gas of $n_g = 100$ cm^{-3} and $v_{\rm dr} = 10$ km s^{-1}, we have according to Huang and Weigert (1982) a minimum distance of

$$d \approx \left(\frac{\dot{m}_w v_w}{4\pi n_g m_g v_{\rm dr}^2}\right)^{1/2} \approx 4 \times 10^{-2} \text{ pc} \tag{6}$$

between the resulting shock front and the star. Very similar results for the effects of radiation pressure and mass loss originating in the Pleiades stars have recently been derived by Gordon and Arny (1984).

Either mechanism or the two in combination is likely to lead to a significant density enhancement at a distance of a few hundredths of a parsec in front of the Pleiades stars. The three-dimensional shape of this density-enhanced region is that of a paraboloid of revolution for which Huang and Weigert (1982) have calculated the geometrical structure. If the axis of such a paraboloidal front is close to the line of sight to the Pleiades, the difference in effective scattering angles for dust situated in the front seen at offsets of 20″ (0.012 pc) and of 40″ (0.024 pc) or 60″ (0.037 pc) would be even greater than for a plane front with $d \approx (1\text{–}5) \times 10^{-2}$ pc.

The values for the distance d derived from equations (5) and (6) are subject to uncertainties of about a factor of 2 or 3. However, both approaches yield predictions for the existence of a front a few hundredths of a parsec from the Pleiades stars, in excellent agreement with the results from the surface brightness of scattered light and with the results from the absorption-line analysis cited earlier.

White (1984*b*), by using a formula which ignored the drag of the gas upon the dust particles, derived minimum dust distances to 17, 20, and 23 Tau about an order of magnitude greater than those derived here, leading to a segregation of dust and the H_2 dissociation and CH^+ formation regions. Our results, based on equations (4) and (5) and on the apparent detection of phase-function effects in the dust-scattered light at small angular offsets, do not support such a segregation of dust and gas; they rather suggest that the molecular gas and the dust coexist even close to the star.

IV. DISCUSSION

If we accept that the reflection nebulosity at small offsets from the Pleiades stars is due mainly to dust at distances of order 10^{-2} pc in front of the stars in the direction to the observer, we must conclude that the effective scattering angle at an offset of 20″ is *smaller* than the effective scattering angle at 40″ or 60″ offset. If we further accept that the dust at these different offsets has the same intrinsic properties, the differences between the relative nebular spectra for the same nebula at different offsets and the deviations of the observed color differences from the theoretical ones computed for wavelength-independent phase functions must be the result of phase-function changes with wavelength. A wavelength-dependent albedo would lead to color differences which are independent of offset distance, and hence this effect can be only of secondary importance here.

In Figure 9 we have plotted the quantity $Q = a(\lambda)/[a(2740)p(\lambda, 2740)]$ under the assumptions of a constant albedo and a phase function given by (Henyey and Greenstein 1941)

$$\Phi_{\rm HG} = (1 - g^2)(1 + g^2 - 2g \cos \alpha)^{-3/2} , \tag{7}$$

with $p[g(\lambda), g(2740)]$ defined by equation (2). In Figure 9 it is assumed that the phase-function asymmetry g at $\lambda = 2740$ Å has the moderate value $g = 0.6$, and it is our goal to examine the conditions under which the Q-values listed in Table 5 could have arisen. The normalization to $g = 0.6$ is not critical here, and the conclusions are qualitatively unchanged as long as $g(2740) \geq 0.5$. Furthermore, the Henyey-Greenstein phase function (eq. [7]) is a simple analytical approximation to the real asymmetric phase function of interstellar dust, and one should not expect agreement in detail other than in gross features. The assumption of a constant albedo is appropriate if the comparison is limited initially to the 1500 Å $\leq \lambda \leq$ 1700 Å region relative to λ2740 (Lillie and Witt 1976). Figure 9 reveals that values $Q \approx 1.5$ found at the larger offsets from 17, 20, and 23 Tau can be achieved by going either to larger values of g, at shorter λ, i.e., from $g = 0.6$ to $g \approx 0.75$, if scattering angles $\alpha \leq 15°$ prevail, or to smaller values of g, i.e., from $g = 0.6$ to $g \approx 0.25$, with correspondingly larger values of α, e.g., $\alpha \geq 70°$. The important distinction arises when one proceeds to smaller offsets, i.e., to smaller scattering angles. In the large-g case smaller scattering angles lead to a still larger value of Q, while in the small-g case a smaller scattering angle leads to a rapid decline of Q. The observed values of Q listed in Table 5 support *only* the second possibility, if foreground dust at a distance of a few × 10^{-2} pc is accepted. As an example, if dust is contained in a plane sheet at $0.02 \leq d \leq 0.04$ pc, scattering angles range as $31° > \alpha_{20''} > 17°$, $50° > \alpha_{40''} > 31°$, and $61° > \alpha_{60''} > 42°$. If the dust front has the paraboloidal shape discussed earlier, the scattering angle at 40″ and 60″ offset can be as large as 70° and 90°.

The values of Q in Table 5 are of order unity for the range 2740 Å $\geq \lambda >$ 2200 Å and are found to increase suddenly for $\lambda <$ 2200 Å for the larger offsets. This can be understood if one takes into account the fact that the observed dust albedo declines between the wavelengths 2740 and 2200 Å (Lillie and Witt 1976; Morgan, Nandy, and Thompson 1976); changes in $a(\lambda)/a(2740)$ are canceled by the opposite change in the phase contribution rate p. Shortward of 2200 Å, however, the two changes will be in the same direction, leading to a mutual reinforcement and a rapid change in Q.

It is our conclusion that the *IUE* spectra of three prominent reflection nebulae in the Pleiades, if interpreted with the best available information about the location of the interstellar matter involved in these nebulae, again indicate that the asymmetry of the scattering phase function in the far-UV is significantly less than the asymmetry applicable to longer wavelengths. This, therefore, supports earlier results of Andriesse, Piersma, and Witt (1977), Witt (1977), and Paper I concerning the Merope nebula. Independent analyses of *IUE* and other data on NGC 7023 (Witt *et al.* 1982) and of *IUE* spectra of NGC 1999 (Cardelli and Böhm 1984), both nebulae with embedded stars, led to the same conclusion.

In terms of particle models we interpret these results as indicating that scattering by small dust particles in the 10^{-6} cm size range plays a much more important role in UV extinction than is usually assumed by currently discussed models.

Only grains with diameters small compared with the wavelength under consideration have scattering phase functions with small asymmetries (e.g., $g \approx 0.25$), but they also have small scattering efficiencies. In a grain-size distribution containing both larger and smaller grains, the relative number of smaller grains must be sufficiently increased, if the small grains, despite their much smaller cross sections and efficiencies for scattering, are to dominate the shape of the scattering phase function.

Independent arguments for the existence of a large populations of grains in the 10^{-7} cm size domain in the general interstellar medium have been advanced by Draine and Anderson (1985) and by Boulanger, Baud, and van Albada (1985) in order to account for *Infrared Astronomical Satellite* (*IRAS*) observations of excess emission at 12 and 25 μm wavelengths from high–galactic latitude interstellar clouds.

Our results are in substantial disagreement with the model calculation of Chlewicki and Greenberg (1984*a*, *b*), who require $0.7 < g < 0.9$ for the far-UV. The alternative model by Mathis, Rumpl, and Nordsieck (1977), equally capable of fitting available extinction and polarization data, predicts $g \approx 0.47$–0.63 for the 2500 Å $> \lambda >$ 1300 Å region (White 1979; Draine and Lee 1984), but the trend with wavelength is opposite that required by our data. If either one of these model predictions were correct, the log (S/F_*) spectrum of the Pleiades nebulae would have to be rising steeply toward shorter wavelength at the smallest offsets, exactly opposite to what is observed. This behavior is not dependent on the exact location of the scattering material in the line of sight to the stars, as long as the material *between* us and the Pleiades is a major contributor to the scattered light.

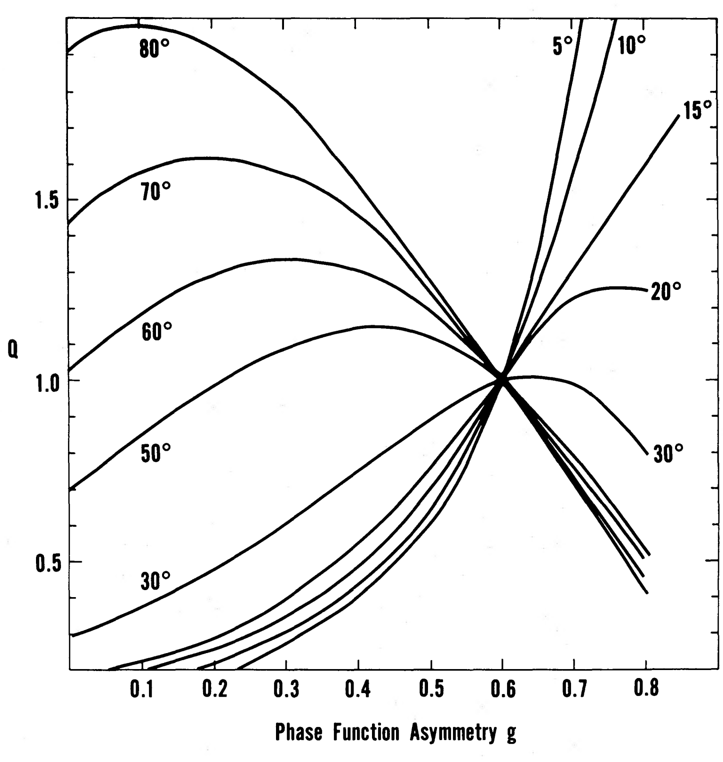

FIG. 9.—The ratio $Q = a(\lambda)/[a(2740)p(\lambda, 2740)]$ has been computed under the assumption of a wavelength-independent albedo. The phase contribution ratio p has been determined from the Henyey-Greenstein phase function, with the asymmetry factor $g(\lambda)$ as the independent variable. The scattering angles occurring in the nebular sheet are indicated next to each curve, and all curves are normalized to $g = 0.6$, the value assumed for $\lambda = 2740$ Å.

V. SUMMARY

1. New *IUE* measurements of the surface brightness of the reflection nebulae associated with the Pleiades stars 17, 20, and 23 Tau have been presented. Each nebula was observed at two offsets, at 20″ (all) and at 40″ (17, 20 Tau) or 60″ (23 Tau) south of the respective illuminating star, and the entire *IUE* wavelength range from 1250 to 3150 Å was covered.

2. After normalization, achieved by dividing the nebular spectra by the spectra of the respective illuminating stars, the resultant log (S/F_*) curves for the three nebulae show the following characteristics in common: At the larger offsets in each instance, S/F_* increases very steeply with decreasing wavelength, and at $\lambda < 2200$ Å it exceeds significantly the values expected on the basis of scattering by grains with a wavelength-independent albedo and phase function. At the smaller offset of 20″ the ratio spectra exhibit a greatly decreased slope in the UV.

3. Arguments based on the interpretation by several authors of interstellar absorption lines seen toward the Pleiades stars, on the interpretation of the surface brightness of scattered light, and on theoretical expectations for the closest approach of a dust front held back by stellar radiation pressure or a shock front held back by a stellar wind yield strong indications that most of the interstellar material seen in the line of sight toward the Pleiades is confined to a thin sheet at a few hundredths of a parsec distance in front of the stars.

4. In this geometry the new *IUE* data can be understood only if the scattering phase function becomes more isotropic with decreasing wavelength throughout the UV observed by the *IUE*.

5. We conclude from this result that the role of scattering by small grains in the 10^{-6} cm size range is very important and that this role is generally underestimated by currently discussed models.

We thank the *IUE* Observatory staff at the Goddard Space Flight Center for their assistance in obtaining the data used for this study. We are particularly grateful to Al Boggess for authorizing the special reprocessing of our data to make them suitable for this analysis. Material support was provided by the National Aeronautics and Space Administration through several grants to the University of Toledo.

REFERENCES

Andriesse, C. D., Piersma, Th. R., and Witt, A. N. 1977, *Astr. Ap.*, **54**, 841.
Arny, T. T. 1977, *Ap. J.*, **217**, 83.
Bohlin, R. C., Lindler, D. J., and Turnrose, B. E. 1981, *NASA/IUE Newsletter*, **12**, 9.
Boulanger, F., Baud, B., and van Albada, G. D. 1985, *Astr. Ap.*, **144**, L9.
Bouvier, P. 1982, in *Compendium in Astronomy*, ed. E. G. Mariolopoulos, P. S. Theocaris, and L. N. Mavridis (Dordrecht: Reidel), p. 43.
Cardelli, J. A., and Böhm, K.-H. 1984, *Ap. J.*, **285**, 613.
Chlewicki, G., and Greenberg, J. M. 1984*a*, *M.N.R.A.S.*, **210**, 791.
———. 1984*b*, *M.N.R.A.S.*, **211**, 719.
Cottrell, M. J., and Witt, A. N. 1983, *A.J.*, **88**, 418.
Draine, B. T., and Anderson, N. 1985, *Ap. J.*, **292**, 494.
Draine, B. T., and Lee, H. M. 1984, *Ap. J.*, **285**, 89.
Duley, W. W., and Williams, D. A. 1980, *Ap. J.* (*Letters*), **242**, L179.
Federman, S. R. 1982, *Ap. J.*, **253**, 601.
Freeman, A., and Williams, D. A. 1982, *Ap. Space Sci.*, **83**, 417.
Gordon, K. H., and Arny, T. T. 1984, *A.J.*, **89**, 672.
Henyey, L. G., and Greenstein, J. L. 1941, *Ap. J.*, **93**, 76.
Huang, R. Q., and Weigert, A. 1982, *Astr. Ap.*, **116**, 348.
Jura, M. 1977, *Ap. J.*, **218**, 749.
———. 1979, *Ap. J.*, **231**, 732.
Lillie, C. F., and Witt, A. N. 1976, *Ap. J.*, **208**, 64.
Martin, P. G. 1978, *Cosmic Dust* (Oxford: Oxford University Press), chap. 8.3.
Mathis, J. S., Rumpl, W., and Nordsieck, K. H. 1977, *Ap. J.*, **217**, 425.
Morgan, D. H., Nandy, K., and Thompson, G. I. 1976, *M.N.R.A.S.*, **177**, 531.
Savage, B. D., and Mathis, J. S. 1979, *Ann. Rev. Astr. Ap.*, **17**, 73.
White, R. E. 1984*a*, *Ap. J.*, **284**, 685.
———. 1984*b*, *Ap. J.*, **284**, 695.
White, R. L. 1979, *Ap. J.*, **229**, 954.
Witt, A. N. 1977, *Pub. A.S.P.*, **89**, 750.
———. 1985, *Ap. J.*, **294**, 216 (Paper I).
Witt, A. N., Bohlin, R. C., and Stecher, T. P. 1981, *Ap. J.*, **244**, 199.
Witt, A. N., and Schild, R. E. 1985, *Ap. J.*, **294**, 225 (Paper II).
Witt, A. N., Schild, R. E., and Kraiman, J. B. 1984, *Ap. J.*, **281**, 708.
Witt, A. N., Walker, G. A. H., Bohlin, R. C., and Stecher, T. P. 1982, *Ap. J.*, **261**, 492.

RALPH C. BOHLIN: Space Telescope Science Institute, Homewood Campus, Baltimore, MD 21218

THEODORE P. STECHER: Code 680, NASA/Goddard Space Flight Center, Greenbelt, MD 20771

ADOLF N. WITT: Ritter Observatory, University of Toledo, 2801 W. Bancroft, Toledo, OH 43606